Supplementary Information for

GSK-3 modulates cellular responses to a broad spectrum of kinase inhibitors

Curtis A. Thorne[1*], Chonlarat Wichaidit[1*], Adam D. Coster[1], Bruce A. Posner[2], Lani F. Wu[1,3,4] and Steven J. Altschuler[1,3,4]

[1]Green Center for Systems Biology, Simmons Cancer Center, University of Texas Southwestern Medical Center, Dallas, TX 75390, USA.

[2]Department of Biochemistry, University of Texas Southwestern Medical Center, Dallas, TX 75390, USA.

[3]Department of Pharmaceutical Chemistry, University of California, San Francisco, San Francisco, CA 94158, USA.

[*]These authors contributed equally to this work.

[4]To whom correspondence should be addressed:

steven.altschuler@utsouthwestern.edu, lani.wu@utsouthwestern.edu

SUPPLEMENTARY RESULTS

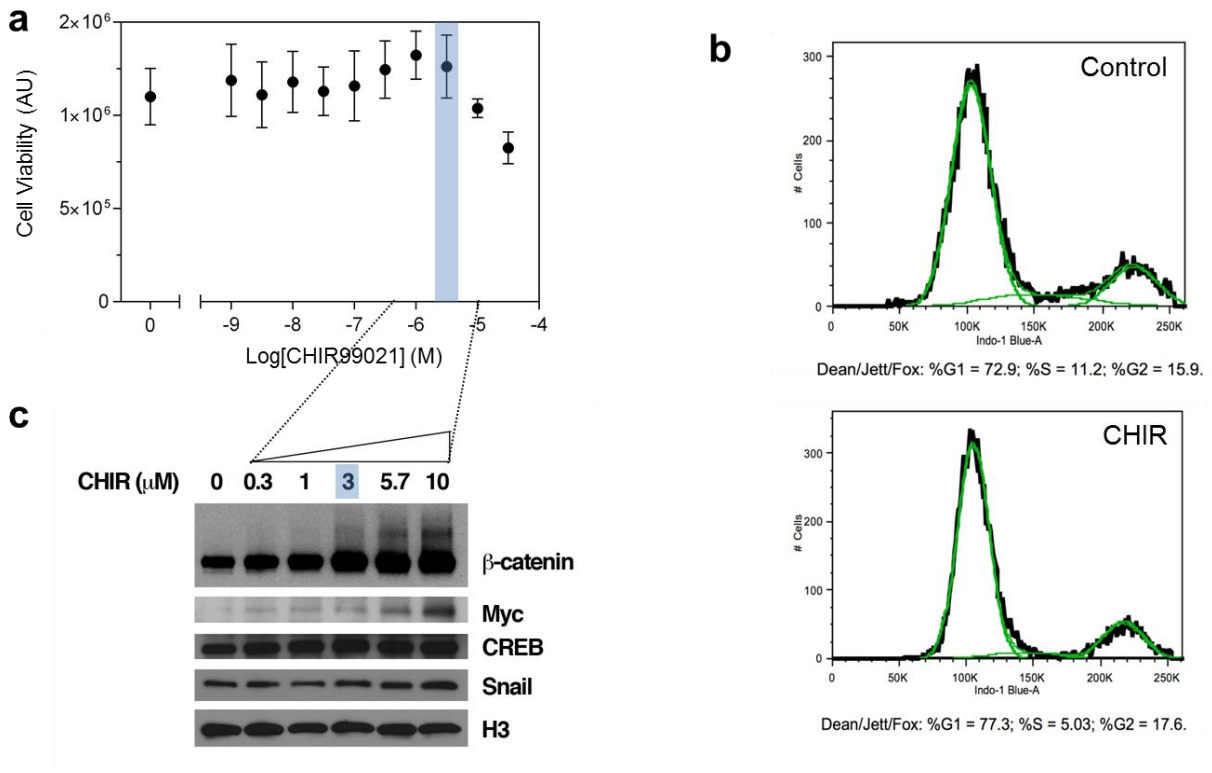

Supplementary Figure 1. 3 μM of CHIR99021 has little effect on cell proliferation and blocks GSK-3-mediated phosphorylation of substrate. (**a**) HCECs were treated with indicated concentration of CHIR99021 for 72 hours and viability observed by measuring cellular ATP levels. Note that 3 μM of CHIR99021 has no significant effect on proliferation in HCECs. (**b**) CHIR treatment for 72 hours did not significantly perturb the cell cycle (c) Effect of CHIR treatments for 48 hrs of HCECs on 4 transcription factor substrates of GSK-3 known to be destabilized by GSK-3 phosphorylation. Note: β-catenin and Myc are stabilized by CHIR with no effect on CREB or Snail. (All of the experiment conditions in panel (**a**) were performed in duplicate. Data represent mean values ± s.d.)

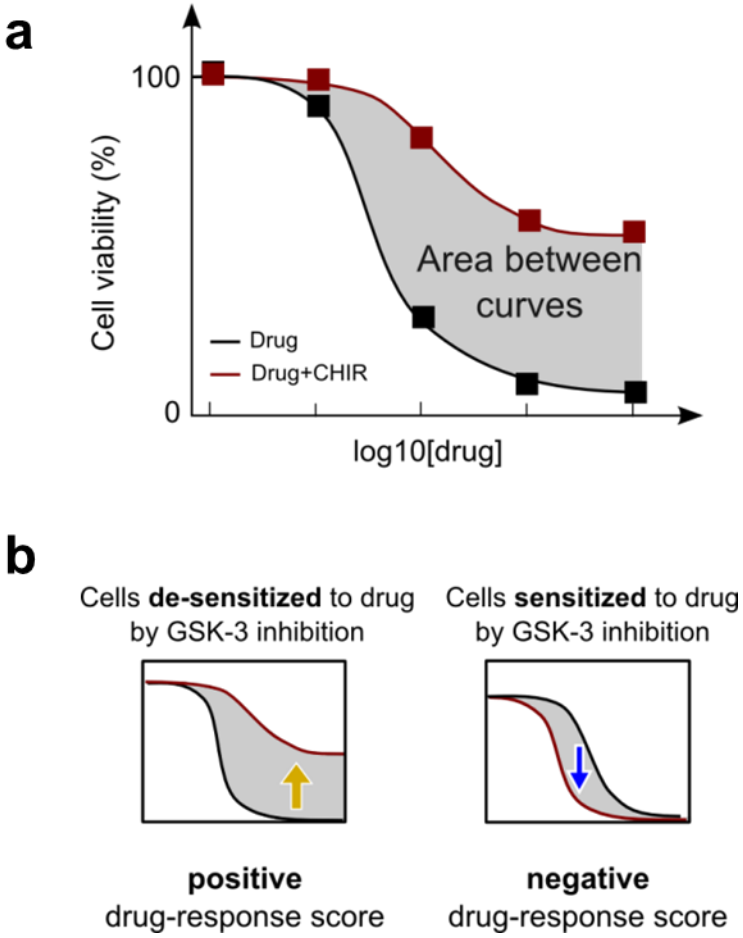

Supplementary Figure 2. Calculation of drug-response score (**a**) Schematic of two drug response curves (**black curve** - drug treatment; **red curve** – drug with 3 μM of CHIR99021 treatment). The drug-response score is calculated by estimating the area between the two response curves (grey area). (**b**) Interpretation of the drug-response score. A positive drug resistance score means a drug becomes less effective when GSK-3 is inhibited, while a negative score means a drug becomes more effective when GSK-3 is inhibited.

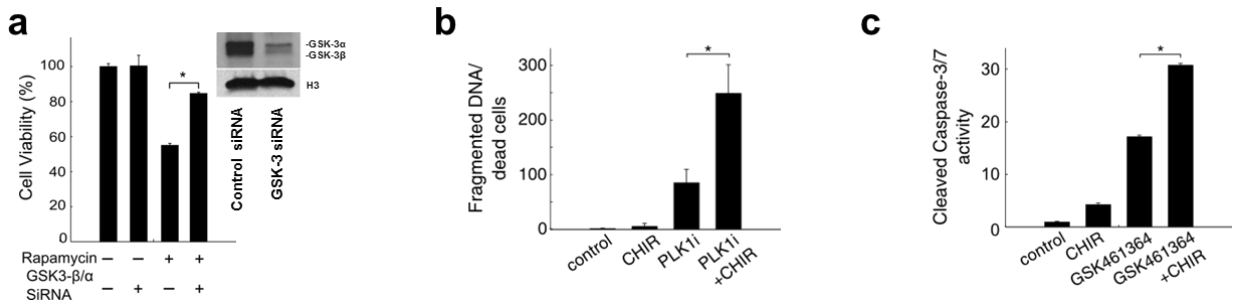

Supplementary Figure 3. GSK-3 inhibition desensitizes cells to mTOR inhibition and sensitizes cells to PLK1 inhibition (**a**) Inhibition of GSK-3 activity via GSK-3 siRNA desensitizes cell to Rapamycin via GSK-3 siRNA. In contrast, inhibition of GSK-3 sensitizes cells to PLK1 inhibition with PLK1 RNAi. We measured either fragmented nuclei after 72 hours treatment (normalized to control) (**b**), or cleaved caspase-3/7 after 48 hours of treatment (normalized to control) (**c**). * Indicates p-values < 0.01. All experimental conditions in (**a**) were performed in duplicate. Data represent mean values ± s.d. See Supplementary Note for (**b**) and (**c**).

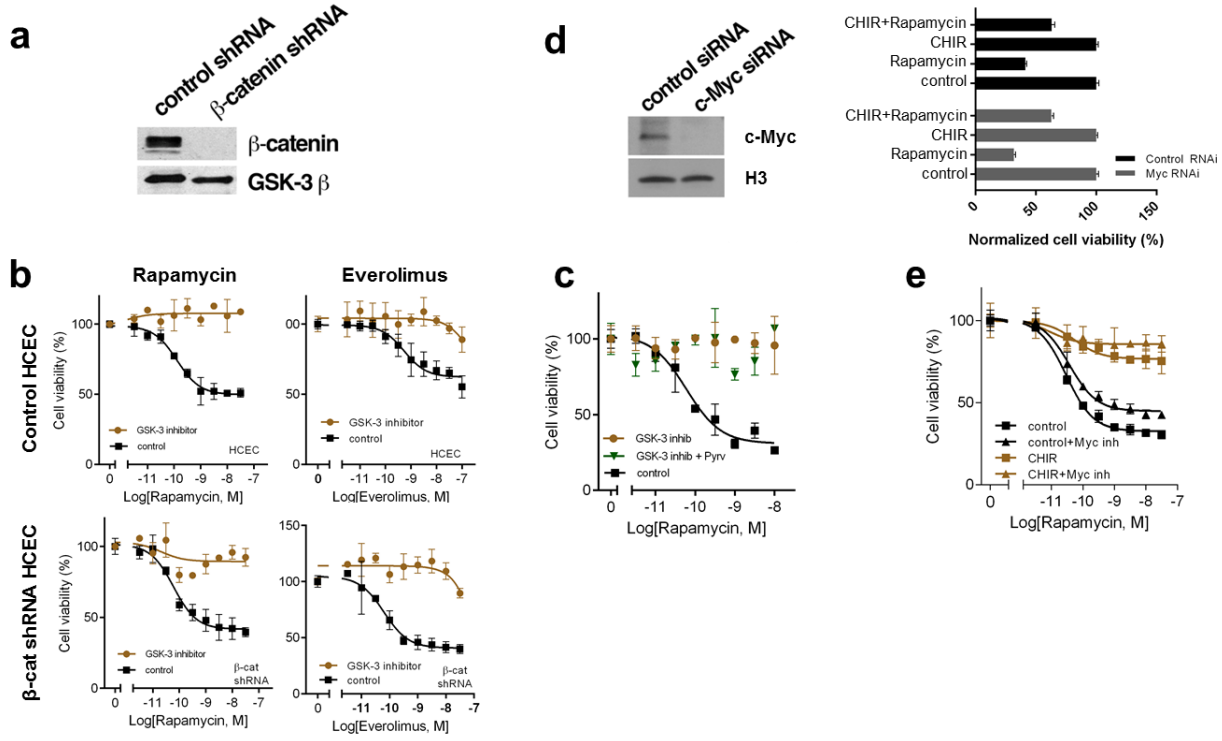

Supplementary Figure 4. Effect of GSK-3 on mTOR-inhibitor sensitivity does not require β-catenin or c-Myc. (**a**) shRNA targeting β-catenin significantly reduces β-catenin protein levels. (**b**) Silencing of β-catenin does not affect CHIR suppression of rapamycin (left panel) and everolimus (right panel) dose-response curves (top panels: control shRNA, bottom panel: β-catenin shRNA). HCECS were treated with anti-β-catenin shRNA for 24 hours and cell viability assays were performed after 72 hours. (**c**) Pyrvinium, a Wnt inhibitor that can block β-catenin signaling downstream of GSK-3, does not block GSK-3-mediated suppression of mTOR inhibitors. **(d)** Silencing of c-Myc does not affect CHIR suppression of rapamycin response. Left panel: western demonstrating effective silencing of c-Myc in a parallel experiment; Right panel: cell viability assay after 72 hr treatment. **(e)** 10058-F4 (50 uM), a Myc inhibitor does not reverse CHIR-mediated suppression of rapamycin. (All the experiment conditions in all panels were performed in duplicate. data represent mean values ± s.d.)

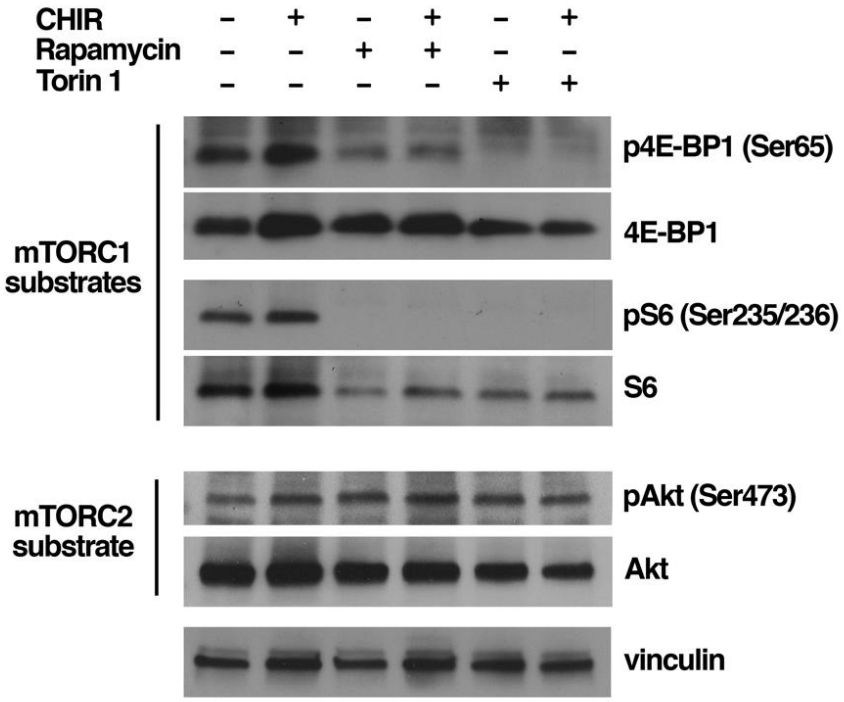

Supplementary Figure 5. GSK3 inhibition blocks mTOR inhibitor response and bypasses outputs of the mTORC1 and mTORC2 complex. GSK-3 inhibition (with CHIR, 3 μM) suppresses Torin 1 and rapamycin-induced cell death but does not reverse blocked phosphorylation of mTORC1 readouts S6 and 4EBP. Additionally, inhibition of GSK-3 does not by pass mTORC1 via activation of the mTORC2 complex as measured by phosphorylation of Akt, an mTORC2 substrate.

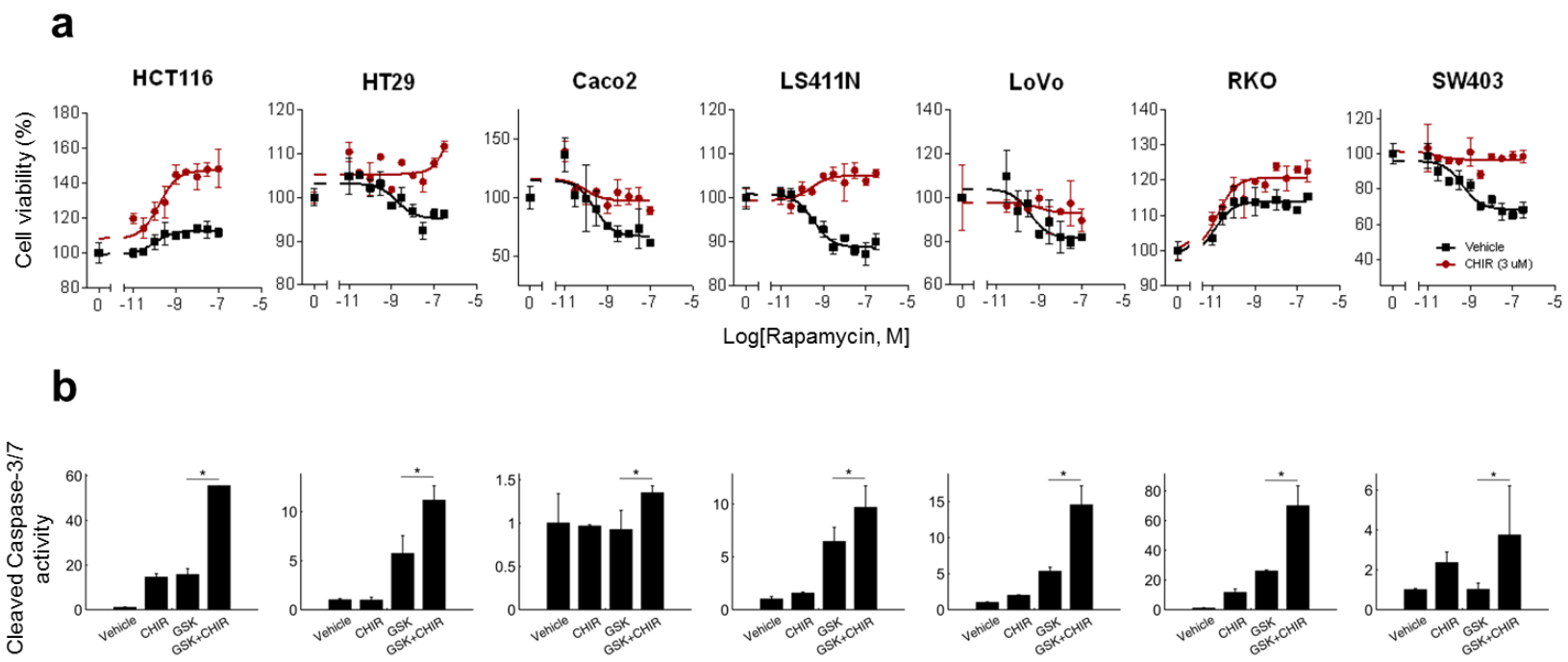

Supplementary Figure 6. GSK-3 inhibition desensitizes colorectal cancer (CRC) cell lines to mTOR inhibitor, and sensitizes CRC cell lines to PLK1 inhibitor. Across panel of 7 CRC lines, GSK-3 inhibition further (**a**) desensitizes CRC cells to rapamycin (72 hours treatment), and (**b**) sensitizes to PLK1 inhibitor GSK4611364 (30nM; 48 hours treatment, cleaved caspase-3/7 activity was observed). * indicates p values < 0.01

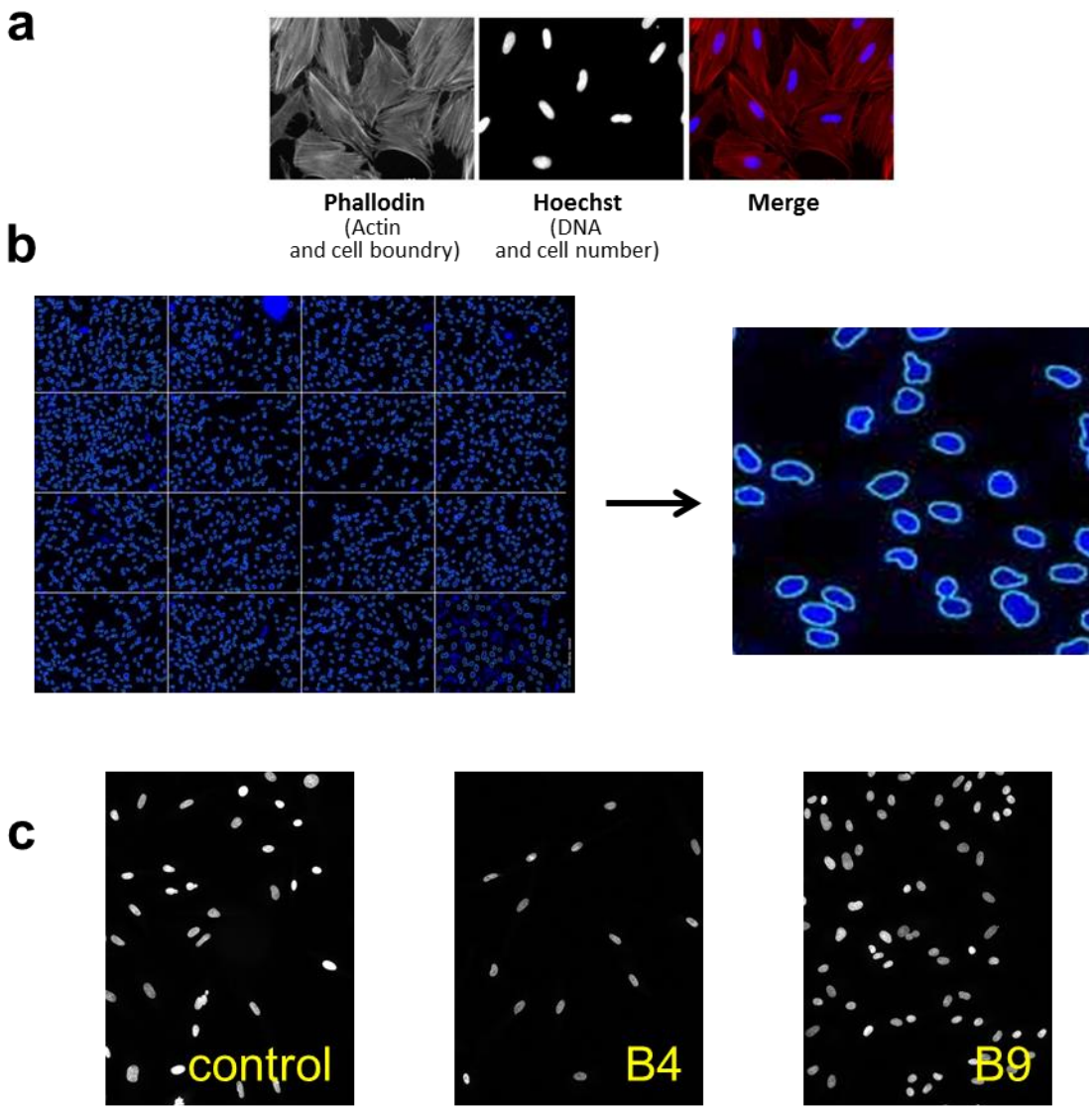

Supplementary Figure 7. High throughput image-based cell viability assay (**a**) Intact cells were identified by staining for DNA and actin, using Hoechst and phallodin, respectively. (**b**) 16 images per well were acquired using automated microscopy and were processed using custom cell-segmentation software to identify single cells (Supplementary information). (**c**) Examples of RNAi-induced death (well B4) or proliferation (well B9).

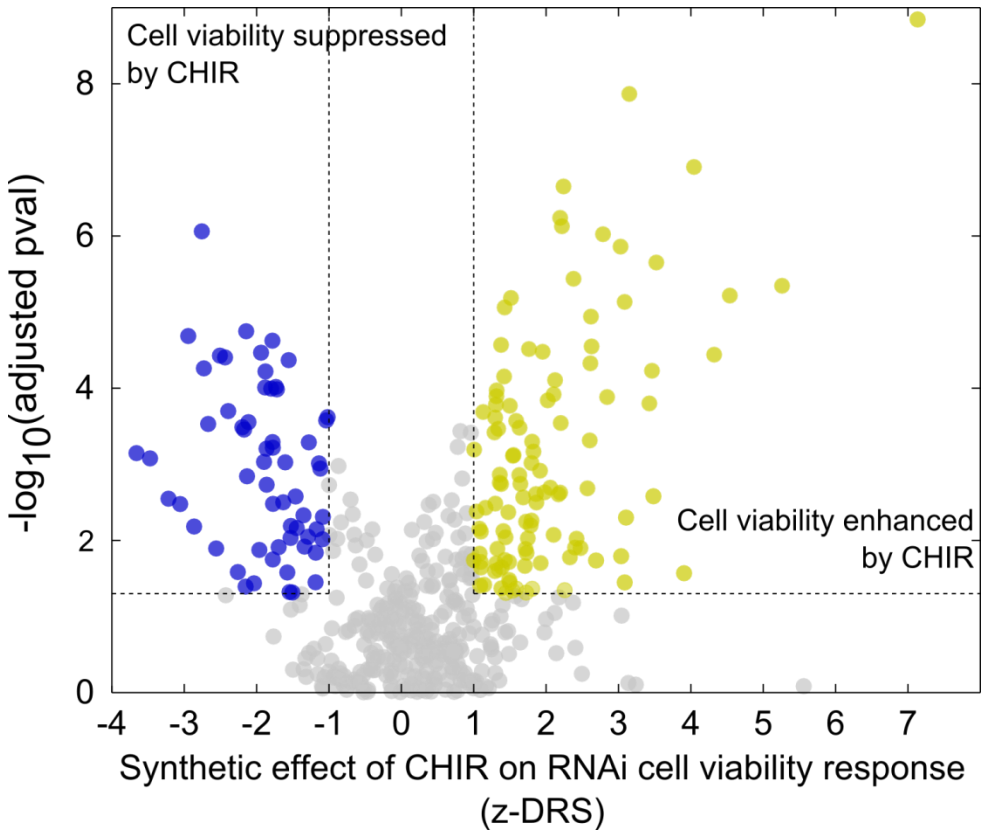

Supplementary Figure 8. **Quantification of synthetic effect of GSK-3 inhibition on RNAi cell viability response**. Volcano plot of GSK-3 modifier screen of the human kinome. X-axis is the ratio of cell count of RNAi+CHIR to RNAi (z-DRS). P-values were calculated from t-tests between triplicates of each RNAi and non-specific RNA. Blue points: (60) genes whose silencing induced increase cell death with GSK-3 inhibition; Yellow points: (115) genes whose silencing increased cell viability with GSK-3 inhibition. The adjusted p-value cutoff was 0.05.

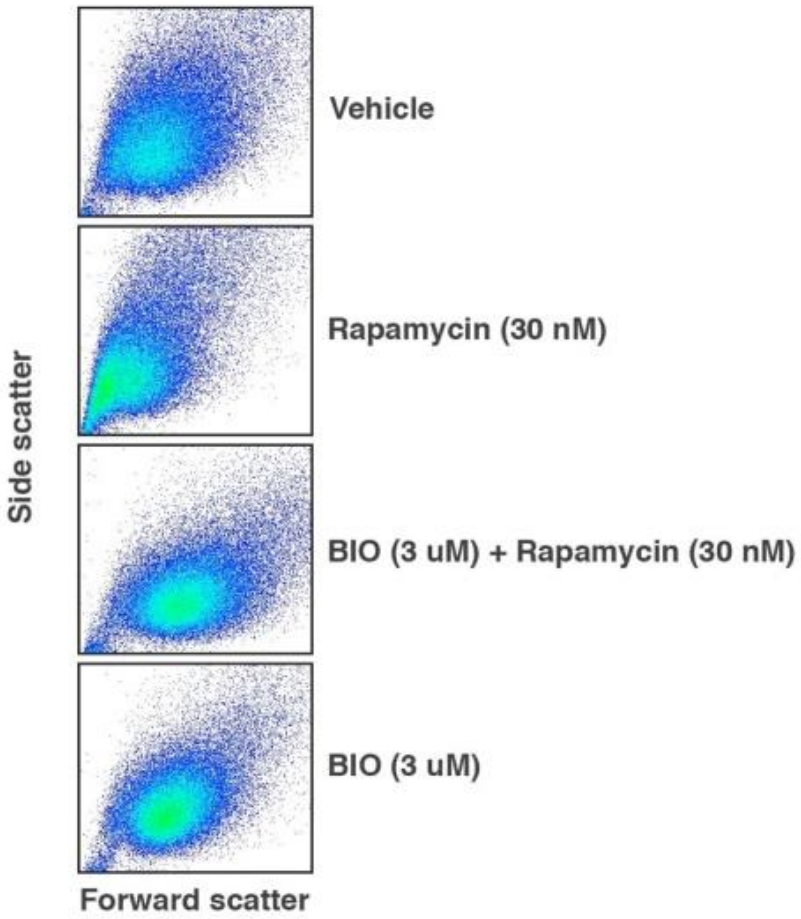

Supplementary Figure 9. GSK-3 inhibition reverses rapamycin-induced decrease in cell volume as measured by flow cytometry. HCECs were treated as indicated and forward and side scatter (surrogates for cell volume) were measured by flow cytometry.

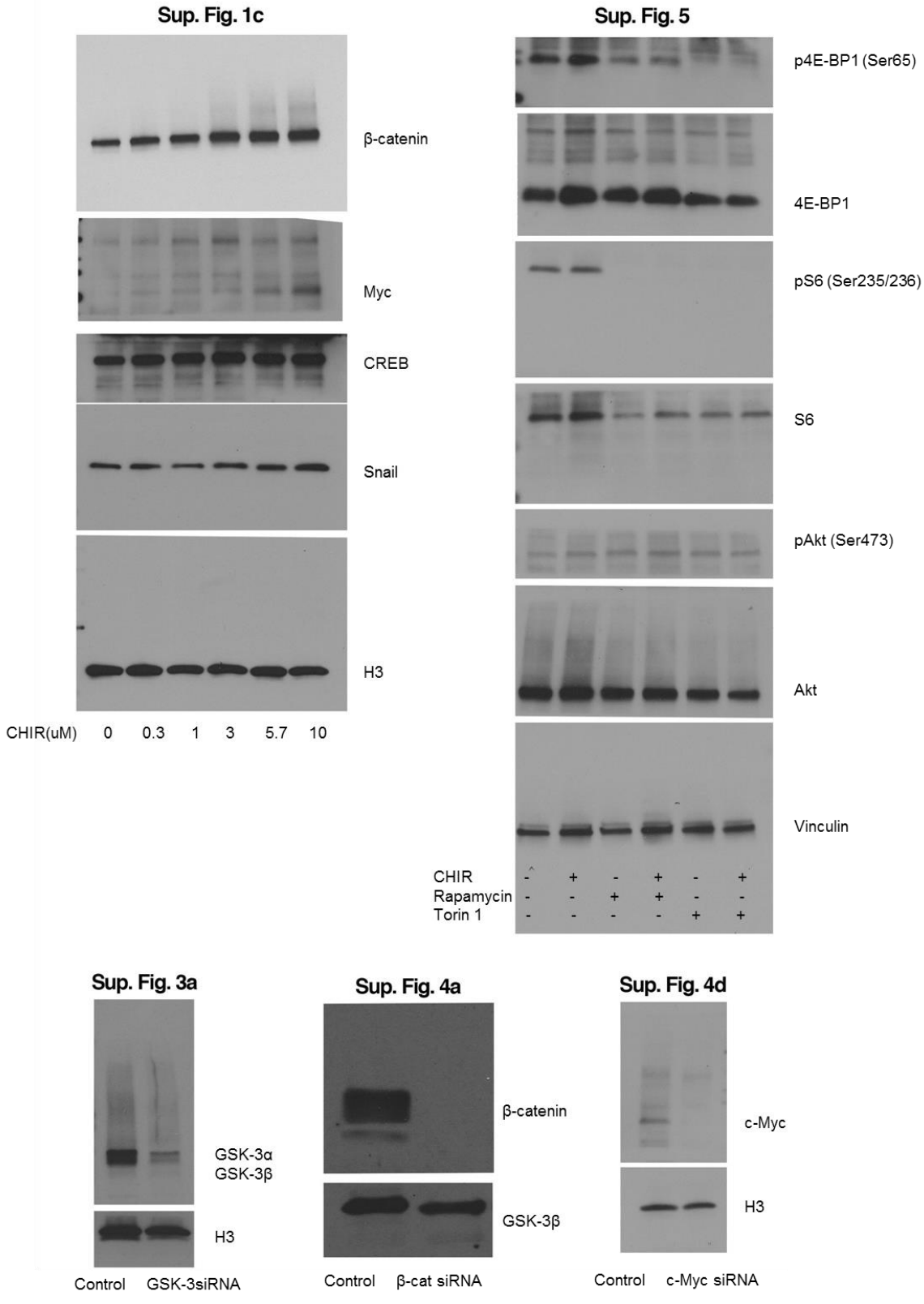

Supplementary Figure 10. Full western blots for all figures.

Supplementary Table 1: Small molecule screening summary

Category	Parameter	Description
Assay	Type of assay	HCECs
	Target	
	Primary measurement	Cell viability (ATP)
	Key reagents	
	Assay protocol	
	Additional comments	
Library	Library size	89 (Oncology set), 376 (GSK-PKIS)
	Library composition	FDA-approved anticaner drugs (Oncology set), Kinase inhibitors (GSK-PKIS)
	Source	NCI (Oncology set), Glaxosmith Kline (GSK-PKIS)
	Additional comments	http://dtp.nci.nih.gov/branches/dscb/oncology_drugset_explanation.html (Oncology set) http://www.maggichurchouseevents.co.uk/bmcs/Downloads/CBDD%20-%20Zuercher%20Bill.pdf (GSK-PKIS) https://www.ebi.ac.uk/chembldb/extra/PKIS/ (GSK-PKIS)
Screen	Format	96-well, BD Falcon 353219
	Concentration(s) tested	0.5%DMSO, 3uM CHIR 7 doses; 0.05-3.2 uM (Oncology set) 7 doses; 0.03-3 uM (GSK-PKIS)
	Plate controls	
	Reagent/ compound dispensing system	
	Detection instrument and software	Envision Multilabel Plate Reader (Perkin Elmer) for cell viability for each dose and all drug, In-house MATLAB script for calculating Drug resistance score (see Supplementary Text)
	Assay validation/QC	
	Correction factors	
	Normalization	
	Additional comments	
Post-HTS analysis	Hit criteria	|Robust Zscore of drug resistance| > 3 Median Absolute Deviation of reference distribution (see Supplementary Text)
	Hit rate	65% (Oncology set), 24% (GSK-PKIS)
	Additional assay(s)	
	Confirmation of hit purity and structure	
	Additional comments	

SUPPLEMENTARY NOTE

1. Drug screen data processing (NCI Oncology Set and GSK-PKIS) (Figure 1)

1.1. GSK-3-dependent drug-response score (DRS)

Dose-response curves to drug treatments (with or without CHIR) were fitted with sigmoidal functions. The area under each curve, denoted AC, was calculated using a trapezoidal integration function. A GSK-3-dependent drug-response score (DRS**)** was defined for area-under-the-curve differences (Supplementary Figure 2):

$$DRS_i = AC_{CHIR+drug_i} - AC_{drug_i}.$$

Note, $DRS_i < 0$ (or $DRS_i > 0$) if CHIR treatment causes drug i to be more sensitive (or resistant) than drug treatment alone.

1.2. Reference distribution

Replicates of rapamycin treatment in every screening plate were used to estimate experimental variability of responses. This provided 6 different dose-response curves, each from a different plate with rapamycin-treated cells. All possible pairs of $AC_{replicate_i} - AC_{replicate_j}$ were computed to give us a "reference" distribution for area-under-the-curve differences of replicate experiments.

1.3. Robust z-score

Using the median, $\tilde{x}_{ref}$, and the median absolute deviation, MAD_{ref}, of the above reference distribution, we transformed our DRS_i into so-called "robust z-score" [1], $z\text{-}DRS_i$, by:

$$z\text{-}DRS_i = \frac{DRS_i - \tilde{x}_{ref}}{MAD_{ref}}.$$

We note that $MAD_{ref} = median\left(abs\left(x_i - \tilde{x}_{ref}\right)\right)$, and recall that the standard deviation and MAD are related for normally distributed data by $\sigma = 1.4826\, MAD$. We refer to this $z\text{-}DRS_i$ as the "GSK-3 dependent drug response robust z-score" in Figure 1.

2. Quantification of nuclei count and average intensity of cleaved caspase-3 (Figure 3, 4 and Supplementary Figure 3, 6)

2.1. Fraction of cell deaths and fragmented nuclei

We manually counted the numbers of fragmented nuclei, dead cells and viable cells from randomly selected control (4 wells) and drug-treated (16 wells) conditions (16 images per well). The number of fragmented DNA was normalized to the total number of cells in each condition, and finally normalized to the control (Fig. 3b, Supplementary Fig. 3b).

2.2. Cleaved caspase-3/7 activity

We identified nuclear regions from DNA-stained cells as previously described[2]. We approximated perinuclear regions by extending nuclear boundaries by 10 pixels. The average Cleaved caspase-3 intensities within nuclear and perinuclear areas were extracted for cells (in 3 replicate wells) for each of the following conditions: DMSO, CHIR, PLK1, and PLK1+CHIR The average cleaved caspase-3/7 intensity from all the conditions were pooled together in one distribution. Next, we obtained the ratio of the number of cells that have average Cleaved caspase-3 intensity higher that the 95th

percentile of the pooled distribution to the total number of cells for each condition. The ratio was then normalized to the control (Fig. 3d, Supplementary Fig. 3c)

Due to difficulty in automatically identifying nuclear regions accurately in many of the colon cancer cell lines due to cell density and overlap, the analysis for caspase-3/7 activity was performed by, first, identifying DNA foreground mask. The foreground masks were obtained from applying a global threshold to each DNA image using Otsu's method[3]. The 95th percentile of caspase-3/7 pixel value was calculated from pooling all the caspase-3/7 pixels (after applying the DNA foreground mask) from all the conditions (control, CHIR, GSK, and GSK+CHIR). Then, we calculated the ratio of number of pixels that have Caspase-3 intensity higher than the 95th percentile to the total number of pixels in DNA foreground mask for each condition (Fig. 3c, 4d).

2.3. Statistical significance test

To test for statistical significance between distributions, we applied Kolmogorov-Smirnov (K-S) tests. Distributions of fragmented DNA (Fig. 3b) and distributions of positive cleaved caspase-3/7 cell (Fig. 3d) for each condition (DMSO, CHIR, GSK and GSK+CHIR) were pooled from roughly 3000 cells for control and CHIR, or 1000 cells for GSK treated conditions. For the panel of CRC lines experiment, K-S tests whereas performed on Caspase-3/7 foreground pixel distributions for GSK treated conditions. We had approximately 2000 cells for each condition.

3. Kinome RNAi screen data processing (Figure 5)

For analyzing our large kinome RNAi screen, we needed to develop an automated approach for estimating cell counts. However, the presence of fragmented nuclei and cell "clumpiness" presented challenges. We describe below our methodology to count cells in each experimental well of a microtiter plate.

3.1. Nuclear identification.

DAPI and phalloidin were used to mark nuclear and cytoplasmic regions (respectively). Nuclear regions were automatically identified [2], and those that were too small to be nuclei (empirically determined to be a cutoff of < 600 pixels) were removed. In each well, we used all 16 images to compute properties of morphology and intensity used below. First, we computed the median area $\tilde{A}_{nuc}$ and median absolute deviation MAD_{nuc} of the regions. Second, we computed the value of the 90th percentile actin or DAPI pixel intensity in each region, defined as I_{90}. We additionally computed a property of each region that told us how round it was to: 1) update cell counts for (larger) clumped nuclei, and 2) remove (smaller) fragmented nuclei. For this purpose, we used a *Regionprops* property in MATLAB called ConvexArea, denoted as $Convex\ A_{nuc}$, which computed the smallest convex hull containing the nuclear region. Subsequently, we calculated a difference between the area of the nuclear region and the convex area: $\Delta A = \frac{Convex\ A_{nuc} - A_{nuc}}{A_{nuc}}$.

Clumped nuclear regions were seen to be both large ($A_{nuc} > \tilde{A}_{nuc} + MAD_{nuc}$) and non-convex ($\Delta A$ value > 0.09). We found that adjusting the cell count from 1 to

$A_{nuc}/(\tilde{A}_{nuc} + MAD_{nuc})$ for the regions satisfying both of the size and convexity criteria gave results that were consistent with visual inspection.

Fragmented nuclear components appeared as small, single, connected multi-lobular regions that tended to have strong intensity in DNA and/or actin staining. Based on these observations, we identified and removed regions that satisfied all three of the following empirically determined criteria: 1) regions that were non-convex ((ΔA value > 0.09); 2) regions whose sizes were less than one MAD deviation away from the median, i.e. $A_{nuc} < \tilde{A}_{nuc} + MAD_{nuc}$; and 3) regions that stained brightly for actin or DAPI nuclear markers (I_{90} is > 90% of the distribution of I_{90}s within the same condition for either DAPI or actin stains).

3.2. Processing of cell count data

Each siRNA treatment was performed in triplicate, each on a separate plate. We analyzed this dataset as follows.

Plate-level normalization (normalized cell count)

We used a plate-level normalization scheme to enable comparison of different siRNA from different plates and conditions [1]. For each plate, p, we normalized the cell count x_j^p of siRNA j treatment by the median cell count of all wells in the plate, $\tilde{x}^p$. That is: $x_{norm}{}_j^p = \frac{x_j^p}{\tilde{x}^p}$.

Well-level correction

To correct for systematic well-specific effects in our siRNA screening process, we took a commonly used strategy [4]. We generated 12 reference plates (6 with DMSO, and 6 with CHIR treatments) to identify well-to-well bias. Using GeneData Screener's proprietary pattern detection algorithm [5], we obtained a corrected factor f_w for each well w. This allowed us to correct the cell count of siRNA *j* treatement performed in well w in plate p as: ${x_{cor}}_j^p = {xnorm_j^p}/{f_w}$.

GSK-3 inhibition effect ratio

For each of our replicate plate pairs ($r = \{1,2,3\}$) treated with siRNA j (p_-^r) or siRNA j + CHIR (p_+^r), we measured the effect of GSK-3 inhibition:

$$E_{j,r} = \frac{{x_{cor}}_{j+CHIR}^{p_+^r}}{{x_{cor}}_j^{p_-^r}}.$$

We obtained a single effect ratio E_j from our three replicates $\{E_{j,r}\}_{r=1}^3$ as previously described[6]. We first computed their median $\tilde{E}_j = median\{E_{j,r}\}_{r=1}^3$ and median absolute deviation $MAD_j = median_{r=1}^3(|E_{j,r} - \tilde{E}_j|)$. In the case when the replicates were tight (i.e. $MAD_j \leq 15\%$), we chose the effect ratio E_j as the median, $\tilde{E}_j$. In the case when replicates were not tight, we chose E_j to be $\tilde{E}_j - MAD_j$ if $\tilde{E}_j < 1$ or $\tilde{E}_j + MAD_j$ if $\tilde{E}_j > 1$. Our choice was motivated by the expectation that a suppressor should result in less cell viability (i.e. $\tilde{E}_j < 1$) and an enhancer should result in more cell viability (i.e. $\tilde{E}_j > 1$).

Reference distribution

In our data, we had a total of 120 negative controls (i.e. non-specific siRNA; 120 with and 120 without CHIR). For each replicate r of these negative controls, we computed its effect ratio $E_{-control,r}$. We pooled all the effect ratios of our negative controls $\{E_{-control,r}\}_{r=1}^{xx}$ to form a reference distribution and computed its MAD_{ref} and $\tilde{E}_{ref}$.

Hit selection

We selected our hits based on two criteria: p-vale and z-score. First, we calculated the p-value p_j for the effect ratio of each siRNA j from a two sample t-test between $\{E_{j,r}\}_{r=1}^{3}$ and $\{E_{-control,r}\}_{r=1}^{12}$ from 12 measurements of the corresponding negative controls (i.e. non-specific siRNA). We then computed the corrected p-value $q_j = \frac{M*p_j}{i}$ for each siRNA j (based on the Benjamini-Hochberg method [7]) where i is the rank of p_j, and M is the total number of siRNA. Second, we computed the $RZscore_j = \frac{E_j - \tilde{E}_{ref}}{MAD_{ref}}$ for all siRNA j. Taken together, we consider siRNA j a "hit" if $q_j < 0.05$ (1.3 in $-log_{10}$ scale), and $|z - DRS_j| > MAD_{ref}$ (Supplementary Figure 8).

4. Mining kinase inhibitors

We utilized DrugBank database [8] to find drugs (either in "investigational" or "approved" categories as defined by DrugBank) that affected the kinases obtained in the previous section (i.e. our "hits"). We found 96 (out of 196) drugs were targeted to 32 (out of 75) the kinases. A summary of these drugs was compiled in Supplementary Data Set 1. We note that our summary also included PLK1 inhibitor, which was found outside DrugBank

and is in phase-3 clinical trials. These 32 targets are indicated in Fig. 5c as red rectangles next to their target in a graphical kinases-GSK-3 interaction.

Glossary

AC: Area under dose response curve

A_{nuc}: nucleus area

CHIR: CHIR99021

$Convex\ A_{nuc}$: convex area

DRS: Drug-response score

MAD: Median Absolute Deviation

$z - DRS$: Robust z-score

Solidity: $A_{nuc}/Convex\ A_{nuc}$

$\tilde{x}$: median of distribution X

SUPPLEMENTARY NOTE REFERENCES

1. Birmingham, A., et al., *Statistical methods for analysis of high-throughput RNA interference screens.* Nat Methods, 2009. **6**(8): p. 569-75.
2. Loo, L.H., L.F. Wu, and S.J. Altschuler, *Image-based multivariate profiling of drug responses from single cells.* Nat Methods, 2007. **4**(5): p. 445-53.
3. Otsu, N., *A Threshold Selection Method from Gray-Level Histograms.* IEEE Transactions on Systems, Man, and Cybernetics, 19791. **9**(1): p. 62-66.
4. Makarenkov, V., et al., *An efficient method for the detection and elimination of systematic error in high-throughput screening.* Bioinformatics, 2007. **23**(13): p. 1648-57.
5. *Genedata M.* 4053 Basel, Switzerland.
6. Kim, H.S., et al., *Systematic identification of molecular subtype-selective vulnerabilities in non-small-cell lung cancer.* Cell, 2013. **155**(3): p. 552-66.
7. Benjamini, Y. and Y. Hochberg, *Controlling the False Discovery Rate - a Practical and Powerful Approach to Multiple Testing.* Journal of the Royal Statistical Society Series B-Methodological, 1995. **57**(1): p. 289-300.
8. Knox, C., et al., *DrugBank 3.0: a comprehensive resource for 'omics' research on drugs.* Nucleic Acids Res, 2011. **39**(Database issue): p. D1035-41.